

Using time reversal symmetry for sensitive incoherent matter-wave Sagnac interferometry

Y. Japha, O. Arzouan, Y. Avishai and R. Folman

Department of Physics, Ben-Gurion University, Be'er-Sheva 84105, Israel

(Dated: May 26, 2019)

We present a theory of the transmission of incoherent guided matter-waves through Sagnac interferometers. Interferometer configurations with only one input and one output port have a property similar to the phase rigidity observed in the transmission through Aharonov-Bohm interferometers in coherent mesoscopic electronics. This property is connected to the existence of counterpropagating paths of equal length and enables the operation of such matter-wave interferometers with incoherent sources. High finesse interferometers of this kind have a rotation sensitivity inversely proportional to the square root of the finesse.

The Sagnac effect, occurring in a wave propagating through a closed rotating ring, induces a phase shift proportional to the angular frequency Ω of this rotation and the area A of the ring [1]. For light waves with frequency ω this phase shift is $\phi_{\text{light}} = (2\omega A/c^2)\Omega$, where c is the speed of light. For de-Broglie waves of non-relativistic particles with mass m , the phase shift is $\phi_{\text{matter}} = (2mA/\hbar)\Omega = (mc^2/\hbar\omega)\phi_{\text{light}}$ [2, 3], so that the rotation sensitivity of a matter-wave interferometer ('ifm') is potentially better by a factor of $\sim 10^{11}$. First experimental attempts demonstrated rotation sensitivities comparable to or even better than those of optical Sagnac ifm's [4, 5, 6]. However, these "one-pass" ifm's are limited by their small effective area and the relatively low flux available from coherent matter wave sources. Light ifm's with "multi-pass" configurations ("high finesse"), such as ring laser gyros, may be used to increase the effective area and achieve good rotation sensitivity. Recently waveguide ring structures for cold atoms were demonstrated [7, 8], opening the door for the development of "multi-pass" guided atomic Sagnac interferometry. However, the small de-Broglie wavelength and short coherence length (of the order of $1\mu m$) of matter waves makes these ifm's very sensitive to imperfections in the guiding potential, leading to effective path length fluctuations.

In this Letter we use the analogy [9] between the Sagnac effect for massive neutral particles and the Aharonov-Bohm (AB) effect in coherent electron transmission through mesoscopic rings [10]. AB ifm's with only two ports connected to the ring show the effect of "phase rigidity" of the transmission pattern as a function of the magnetic flux Φ , when an effective path length difference between the ifm arms is introduced [11, 12]. The locking of the transmission pattern at $\Phi = 0$ stems from the time reversal invariance and current conservation properties of any system with two ports, which implies that transmissivity is invariant to magnetic field inversion $\Phi \rightarrow -\Phi$. We show that this property, when applied to matter wave Sagnac ifm's, leads to their robustness under effective path length differences and enables their operation in a high finesse configuration and

with incoherent sources, which are available with higher particle flux. Ifm's of this kind will enable increasing the rotation sensitivity and their miniaturization onto atom chips [13] while maintaining the required sensitivity.

In general, a Sagnac ifm consists of a loop and one or more junctions, each consisting of one or more beam splitters (BS) connecting the loop to input and output channels. Here we consider a one dimensional (1d) model in which the particles are guided in a single transverse mode of the waveguide. A linear junction with n ports is represented by a $n \times n$ unitary scattering matrix S connecting the output amplitudes to the input amplitudes at the ports. As demonstrated in fig.1 we denote the indices of the ports of the input junction connected to the ifm loop by α and β and the ifm input port by i . The corresponding input and output amplitudes at the internal ports α and β will be denoted by a_{\pm} and b_{\pm} respectively and the ifm input amplitude by a_{in} (normalized to $a_{in} = 1$). The relation between the amplitudes is then given by

$$\begin{pmatrix} a_+ \\ b_+ \end{pmatrix} = \begin{pmatrix} S_{\alpha i} \\ S_{\beta i} \end{pmatrix} a_{in} + \begin{pmatrix} S_{\alpha\alpha} & S_{\alpha\beta} \\ S_{\beta\alpha} & S_{\beta\beta} \end{pmatrix} \begin{pmatrix} a_- \\ b_- \end{pmatrix}. \quad (1)$$

If the system is linear, then the amplitudes a_-, b_- are related to the amplitudes a_+, b_+ by

$$\begin{pmatrix} a_- \\ b_- \end{pmatrix} = S_L \begin{pmatrix} a_+ \\ b_+ \end{pmatrix} \quad (2)$$

where the 2×2 S -matrix $S_L(k, \Omega)$ describes the transmission through the loop, thereby containing terms of the form $e^{i(kL \pm \phi)}$, $\hbar k$ being the longitudinal momentum of the particles, L the circumference of the loop and ϕ the rotational phase shift. S_L is in general non-unitary when particles can leave the loop from another junction. Time reversal symmetry (Onsager relations [14]) implies that $S_{\alpha\beta} = S_{\beta\alpha}$ and that S_L has the form $S_L = \begin{pmatrix} a & be^{i\phi} \\ be^{-i\phi} & c \end{pmatrix}$, where a, b and c are functions of k . By combining eqs. (1) and (2) we find the solution

$$\begin{pmatrix} a_+ \\ b_+ \end{pmatrix} = \frac{1}{I-T} \begin{pmatrix} S_{\alpha i} \\ S_{\beta i} \end{pmatrix} a_{in} = \sum_{n=0}^{\infty} T^n \begin{pmatrix} S_{\alpha i} \\ S_{\beta i} \end{pmatrix} \quad (3)$$

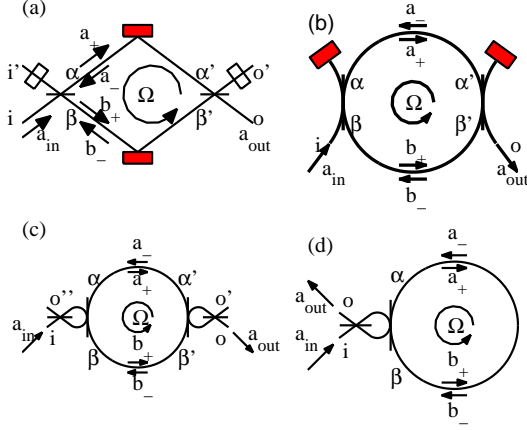


FIG. 1: Geometries of guided matter-wave Sagnac interferometers: (a) MZ. Open squares mean controllable reflectivity. When fully reflecting we name the ifm: closed MZ. (b) 2-port loop. Closed squares are fully reflecting mirrors. (c) 4-port loop. (d) single junction loop. In all configurations horizontal lines mean 50-50% BSs while vertical lines mean BSs with a transmission amplitude it .

where I is the 2×2 unity matrix and $T = \tilde{S}S_L$, \tilde{S} being the sub-matrix of S appearing in eq. (1). The output of the ifm is obtained when propagating the amplitudes a_+, b_+ through the ifm arms and transmitting them into the output port through the output junction. When no additional imperfections exist in the arms, the output amplitude is given by

$$a_{out} = S'_{o\alpha'} e^{i(k-\phi/L)L_\alpha} a_+ + S'_{o\beta'} e^{i(k+\phi/L)L_\beta} b_+, \quad (4)$$

where S' is the scattering matrix of the output junction and L_α, L_β are the lengths of the corresponding arms, such that $L = L_\alpha + L_\beta$.

Time reversal symmetry, which determines the symmetry properties of the scattering matrices \tilde{S} and S_L discussed above yields the following general form of the transmission through the ifm [12]

$$P(k, \phi) = |a_{out}|^2 = \frac{B + C \cos(\phi + \beta)}{1 + D \cos \phi + H \cos^2 \phi}, \quad (5)$$

where B, C, D, H and β are functions of k . When the ifm has only one input and one output port, time-reversal symmetry and current conservation imply that $P(\phi) = P(-\phi)$ so that $\beta = 0$ or $\beta = \pi$ ("phase rigidity"). In what follows we show that while in an ifm having more than two open ports β may be strongly k -dependent, such that an integration over a wide momentum bandwidth Δk washes out the ϕ dependence of $P(\phi)$, this dependence is conserved in an ifm having only 2 open ports and fixed β , enabling wide momentum bandwidth operation.

Let us first examine a simple Sagnac ifm which does not satisfy the condition for "phase-rigidity". The Mach-Zehnder (MZ) ifm shown in fig.1a is analogous to the

ifm implemented in [6]. It contains two 50-50% junctions where an incident particle may be either reflected with amplitude $S_{\beta,i} = S_{\alpha,i'} = 1/\sqrt{2}$ or transmitted with amplitude $S_{\alpha,i} = S_{\beta,i'} = i/\sqrt{2}$. This is a one-pass ifm, where no reflections occur from the loop ports α and β back into the loop ($\tilde{S} = S_L = T = 0$), so that the transmission probability at the output port o is $P(k, \phi) = \sin^2[(\phi - k\delta L)/2]$, where $\delta L = L_\alpha - L_\beta$ is the length difference between the ifm arms. $P(k, \phi)$ can be then written in the form (5) with $B = -C = 1/2$, $D = H = 0$ and $\beta = k\delta L$. If $\delta L \neq 0$ and the input flux is described by a Gaussian spectral distribution $G(k)$ with bandwidth Δk around $k = \bar{k}$, then the time-averaged transmission probability $P(\Omega) = \int dk G(k) P(k, \phi(\Omega))$ becomes

$$P(\Omega) = \frac{1}{2} \left[1 - \eta \cos \left(\frac{2mA}{\hbar} \Omega - \bar{k}\delta L \right) \right] \quad (6)$$

where the interference visibility $\eta = e^{-\Delta k^2 \delta L^2 / 2}$ decreases with momentum bandwidth and path difference. If, in addition, the atomic beam is not perfectly collimated so that parts of it take paths surrounding different effective area with uncertainty δA , then η is multiplied by a factor $\exp[-(2m/\hbar)^2 \delta A^2 \Omega^2 / 2] = \exp[-(\delta A^2 / A^2) \phi^2 / 2]$. Both suppression factors have been observed experimentally, as demonstrated in fig.3 of ref. [6].

In contrast, we now study a closed loop ifm obtained by closing the ports i' and o' of the MZ with mirrors placed in front of them (fig.1a), so that each junction now has only 3 open ports. A particle incident from one of the loop arms on such a junction may be reflected back into the loop with amplitude $S_{ij} = e^{i\varphi_{ij}}/2$, where each phase φ_{ij} ($i, j = \alpha, \beta$) consist of a contribution θ upon reflection at the mirror and an additional $\pi/2$ phase for each transmission through the BS. We then have $S_{\alpha\alpha} = -S_{\beta\beta} = e^{i\theta}/2$ and $S_{\alpha\beta} = S_{\beta\alpha} = ie^{i\theta}/2$. The matrix S_L has elements similar to the elements of the S -matrix of the output junction, $(S_L)_{ij} = S'_{ij} e^{i\eta_{ij}}$, where η_{ij} describe propagation through the arms: $\eta_{ij} = kL \pm \phi$ for $i \neq j$ and $\eta_{jj} = 2kL_j$. Following the above prescription, we obtain the transmission probability as in (5) with $\beta = 0$, such that $P(\phi) = P(-\phi)$. In order to study the properties of the transmission when the source has a momentum bandwidth Δk , it is insightful to realize, in view of eqs. (3) and (4), that the output amplitude can be written as a sum $a_{out} = \sum_{n=0}^{\infty} a_n e^{i(n+1/2)kL}$, where the amplitudes a_n are functions of k with terms $e^{ik\delta L}$, which are slowly oscillating relative to the fast oscillation of e^{inkL} , if we assume small path length differences $\delta L \ll L$. In the transmission probability $P(k, \phi) = |a_{out}|^2$ these fast oscillations will appear in cross terms $a_n^* a_{n'}$ with $n \neq n'$ describing interference between trajectories with different number of passes through the loop in either direction. In a realistic situation where the coherence length of the matter-wave source is much smaller than L ($\Delta k \gg 2\pi/L$), these interference terms will be eliminated. We

describe this elimination by defining a slowly varying time-averaged transmission probability integrated over a period $2\pi/L$ of the fast oscillations

$$\bar{P}(k, \phi) \equiv \left(\frac{L}{2\pi} \right) \int_{k-\pi/L}^{k+\pi/L} dk' |a_{out}(k', \phi)|^2 \approx \sum_{n=0}^{\infty} |a_n|^2, \quad (7)$$

which describes the transmission of a quasi-monochromatic flow ($\Delta k \delta L \ll 1$), where the coherence length is large enough relative to effective path length differences between trajectories with the same number of passes. In the incoherent limit where $\Delta k \delta L \gg 1$, integration of $P(k, \phi)$ over the bandwidth is equivalent to taking the average of \bar{P} over $0 < k \delta L < 2\pi$. In this limit only paths with exactly the same length may interfere.

For the closed MZ the transmission probability in the quasi-monochromatic case is found to be

$$\bar{P} = \frac{1 - 1/2(\cos^2 k \delta L + \cos^2 \phi)}{1 - 1/4(\cos k \delta L - \cos \phi)^2}, \quad (8)$$

as shown in fig.2a for a few values of $k \delta L$ (thin curves). In the incoherent limit (thick curve) the visibility is not suppressed as in the simple MZ but stays fixed at $\eta \approx 0.16$. A more general explanation for this residual visibility is interference between counterpropagating waves that follow trajectories with exactly equal length, as in white light interferometry. Change of the rotation frequency Ω changes the relative phase between these trajectories but they still interfere. In the closed MZ the existence of such pairs of interfering trajectories is allowed by internal reflections, which in a system with a single transverse mode are an inevitable result of current conservation in a junction with only three ports.

The rotation sensitivity of a Sagnac ifm is the minimal rotation frequency change $\delta\Omega_{min}$ that generates a noticeable transmission change (beyond noise level). For an average incident flux F with a Poissonian particle number distribution

$$\delta\Omega_{min} = \frac{\hbar}{2mA} \frac{\delta\phi_{min}}{\sqrt{F\tau}}, \quad \delta\phi_{min} = \sqrt{P(\phi)} \left| \frac{\partial P}{\partial \phi} \right|^{-1}, \quad (9)$$

where τ is the measurement integration time and $\delta\phi_{min}$ the dimensionless phase sensitivity per particle. The best sensitivity is achieved approximately near points with maximal derivative of the transmission. For ifm's with sinusoidal transmission as the MZ, the best sensitivity is inversely proportional to the visibility η .

In order to achieve better rotation sensitivity we now turn our attention to ifm's with a high finesse loop, where the finesse (\mathcal{F}) is defined as the ratio between the periodicity of the spectral transmission $2\pi/L$ and the resonance bandwidth $(1-R)/\sqrt{RL}$, R being the probability to stay in the loop for a full round-trip. For a high finesse loop ($R \approx 1$), \mathcal{F} is proportional to the average number

of passes of a particle through the loop before exiting through a junction. The closed MZ ifm can be converted into a high finesse ifm by replacing the BS of the closed MZ with a "vertical" BS rotated by 90° relative to the MZ BS (fig.1b). A particle incident on the "vertical" BS has a reflection amplitude r and a transmission amplitude $it = i\sqrt{1-r^2}$, which is controllable, for example, with a magnetic tunneling barrier as suggested in [15]. $\mathcal{F} \gg 1$ requires that $r \approx 1$ and $t \ll 1$. Here the transmission amplitude between the two arms $S_{\alpha\beta} = S_{\beta\alpha} = r$, while back reflection through the mirror is only permitted to arm $\beta\beta'$ with amplitude $S_{\beta\beta} = -t^2 e^{i\theta}$. An analysis similar to that of the closed MZ yields the quasi-monochromatic transmission probability shown in fig.2b for different values of $k \delta L$ (thin curves). The transmission has a symmetric dip at $\phi = 0$, whose depth and width depends on the value of $k \delta L$. Its width for a given value of $k \delta L$ is proportional to the spectral bandwidth $\Delta_k = (1-r^4)/r^2 L \approx 2t^2/rL$ of the loop, which is inversely proportional to its finesse $\mathcal{F} = (2\pi/L)/\Delta_k \approx \pi r/t^2$. In the incoherent limit (thick curve), $\bar{P}(\phi) \approx P_0[1 - \eta\mathcal{L}(\phi)]$, where $P_0 \approx t^2/r$, $\mathcal{L}(\phi)$ is a Lorentzian of FWHM $\Delta_\phi \sim \Delta_k L$ and $\eta \approx 0.175$. Using eq. (9), the best sensitivity near $\phi \approx \pm\Delta_\phi/2$ is $\delta\phi_{min} \sim \Delta_\phi/\sqrt{P_0}/\eta \approx \sqrt{2\Delta}/\eta_\phi \propto \mathcal{F}^{-1/2}$. The transmission dip at $\phi = 0$ is due to the fact that interference between pairs of equal length paths terminating at the output port is destructive when $\phi = 0$. For comparison, we calculated the transmission of a similar high finesse ifm with additional ports using a combination of a 50-50% BS and a "vertical" BS at each junction (fig.1c). The quasi-monochromatic transmission of this ifm (thin curves in fig.2c) is not symmetric about $\phi = 0$ and the visibility drops to 0 in the incoherent limit (thick curve).

Finally we utilize the formalism developed here to analyze a simple ifm where each trajectory has a counter-propagating counterpart of the same length. The ifm configuration in fig.1d contains only one junction for input and output. Its output amplitude is obtained by substituting $L_\alpha = L_\beta = L$ and $S' = S$ in eq. (4). The matrix T for this ifm is diagonal, corresponding to no coupling between counterpropagating modes, but on the other hand, all trajectories of the same order n have exactly the same length, giving rise to destructive interference at $\phi = 0$. The slowly varying transmission probability (7) is then a sum over k independent contributions $t^4 r^{2n} \sin^2[(n+1)\phi]$ resulting in

$$\bar{P}(\phi) = \frac{t^2}{1+r^2} \left[1 - \frac{\cos^2 \phi}{1 + 4(r/t^2)^2 \sin^2 \phi} \right] \quad (10)$$

with a Lorentzian dip at $\phi = 0$ of FWHM $\Delta_\phi = t^2/r$, full visibility ($\eta = 1$) and an asymptotic transmission $P_0 \approx t^2/2r$, as shown in fig.2d (thick curve). The best sensitivity at $\phi \rightarrow 0$ is $\delta\phi_{min} \approx t/(2\sqrt{2r}) = \sqrt{\Delta_\phi/2}/2$, which scales as the inverse square root of the finesse $\mathcal{F} = 2\pi r/t^2$. The transmission visibility is not affected by

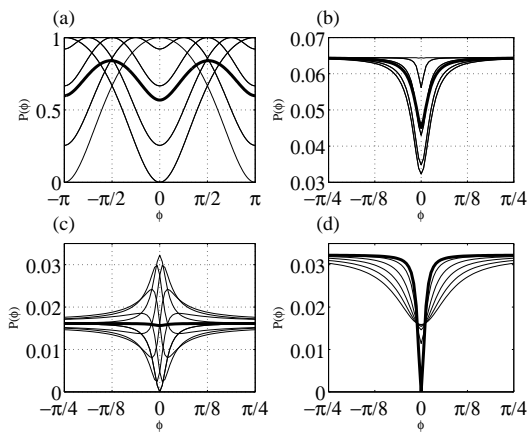


FIG. 2: Transmissivity of Sagnac ifm's as a function of rotational phase shift ϕ (a) closed MZ. (b) 4-port loop. (c) 2-port loop. (d) single junction loop. Thin curves in plots (a-c) represent the quasi monochromatic transmission $\bar{P}(\phi)$ for few values of phase difference between the two arms $k\delta L$, and in plot (d) the transmission in the presence of a scattering center at $x = L/3$ with reflection amplitudes from $r = 0$ (thick curve) to $r = 0.25$. Thick curves in (a-c) represent the transmission in the incoherent limit while all curves in (d) apply both in the quasi monochromatic and the incoherent limit. For all four models $t = 0.25$. As can be observed, the phase locking in (c) suppresses the asymmetric functions appearing in (b), giving rise to less smearing of the interference pattern. The final dip in the incoherent signal of (c) may be explained as interference only between exact same length trajectories, which due to the $\pi/2$ phase difference between the r and t amplitudes, give rise to destructive interference.

changes in the effective path length, but may be affected by internal reflections from asymmetrically located imperfections in the guiding potential. This effect may be calculated from eq. (3) when the effect of scattering centers is included in the loop S_L matrix. As an example, we present in fig.2d the incoherent transmission of the ifm when a single scattering center with reflectivity amplitude $0 \leq r \leq 0.25$ is placed at $x = L/3$. The sensitivity is then degraded both by visibility reduction and increase of the Lorentzian width, while the minimum transmission point stays at $\phi = 0$. The effect of a non-dispersive scattering center (which does not change the effective path length) is similar for other high finesse ifm's discussed above, regardless of their phase rigidity property.

To get an estimate of the achievable sensitivity of a Sagnac ifm on an atom chip, we assume that an atom waveguide ring of radius 1cm is formed near the chip by magnetic field gradients of the order $|\nabla\mathbf{B}| \sim \text{G}/\mu\text{m}$, which may be generated by wires on the chip, about $10\mu\text{m}$ from the surface. The centrifugal force mv^2/r of the circulating atoms must not exceed $\mu_B|\nabla\mathbf{B}|$. This limits the maximum velocity of the atoms to $v \sim 10\text{m}/\text{sec}$. An atomic trap lifetime of about 10s permits up to 1000-2000 rotations, corresponding to a tunneling amplitude

$t \sim 0.035$ at the BS. For the single junction loop we obtain $\delta\phi_{\min} \sim 0.013$. If we assume a flux of 10^9 atoms per second (e.g. from a 2d MOT [16]) we obtain a sensitivity of $\delta\Omega \sim 5 \cdot 10^{-13} \text{rad}/\text{sec}/\sqrt{\text{Hz}}$ - about three orders of magnitude better than the best value published to date [17].

The 1d waveguide model put forward above can be easily extended to a multi-mode model where a waveguide supports $N > 1$ transverse modes. We then have to replace the amplitudes a_{in}, a_{out}, a_{\pm} and b_{\pm} with N component vectors and the matrices \bar{S}, S_L and T with $2N \times 2N$ matrices, which may also couple between the modes. The application of the suggestions in this Letter to real systems requires a more comprehensive study of the multi-mode case as well as other important effects, such as dispersion of ifm components, Berry's phase in a magnetic ring potential [18] and atom-atom collisions. The ideas raised in this work concerning time reversal symmetry in a rotating quantum system with many possible paths are closely related to the theory of weak localization and coherent back scattering in mesoscopic electronic systems in the presence of a magnetic field[10].

We thank Daniel Rohrich, Ora Entin-Wohlman and Amnon Aharony for useful discussions. R.F. would like to sincerely thank Yoseph (Joe) Imry, for years of inspiration and specifically for his insight into quantum mechanics and interferometry. We gratefully acknowledge the support of the European Union FP6 'atomchip' (RTN) collaboration, the German Federal Ministry of Education and Research (BMBF-DIP project), the American-Israeli Foundation (BSF) and the Israeli Science Foundation.

-
- [1] For a recent review, see I. A. Andronova and G. B. Mal'kin, Phys. Usp. **45**, 793 (2002)
 - [2] F. Hasselbach, M. Nicklaus Phys. Rev. **A 48** 143 (1993)
 - [3] S. A. Werner, J-L. Staudenmann, R. Colella, Phys. Rev. Lett. **42** 1103 (1979)
 - [4] F. Riehle et. al., Phys. Rev. Lett. **67** 177 (1991)
 - [5] A. Lenef et al. Phys. Rev. Lett. **78** 760 (1997)
 - [6] T. L. Gustavson, P. Bouyer, M. A. Kasevich, Phys. Rev. Lett. **78** 2046 (1997)
 - [7] A. S. Arnold, C. S. Garvie and E. Riis, Phys. Rev. **A 73**,041606 (2006)
 - [8] I. Lesanovsky et. al., Phys. Rev. **A 73**, 033619 (2006)
 - [9] J. J. Sakurai, Phys. Rev. **D 21**, 2993 (1980)
 - [10] Y. Imry, Introduction to Mesoscopic Physics, Oxford University Press 1997
 - [11] M. Büttiker, Phys. Rev. Lett. **57**, 1761 (1986); A. Levy Yeyati and M. Büttiker, Phys. Rev. **B 52**, R14360 (1995)
 - [12] A. Aharony, O. Entin-Wohlman, B. I. Halperin and Y. Imry, Phys. Rev. **B 66**, 115311 (2002)
 - [13] R. Folman et. al., Adv. At. Mol. Opt. Phys. **48**, 263 (2002); J. Reichel, Appl. Phys. B **74**, 469 (2002)
 - [14] L. Onsager, Phys. Rev. **38**, 2265 (1931); H. B. G. Casimir, Rev. Mod. Phys. **17**, 343 (1945);
 - [15] E. Andersson, M. T. Fontenelle and S. Stenholm, Phys.

Rev. **A 59**, 3841 (1999)

[16] J. Schoser et. al., Phys. Rev. **A 66**, 023410 (2002)

[17] T. L. Gustavson, A. Landragin and M. A. Kasevich,

Class. Quant. Grav. **17**, 2385 (2000)

[18] P. Zhang and L. You, arXiv:quant-ph/0610225 (2006)